Biochimica et Biophysica Acta 1838 (2014) 2817–2824

Contents lists available at ScienceDirect

Biochimica et Biophysica Acta

journal homepage: www.elsevier.com/locate/bbamem

Improving the apo-state detergent stability of NTS_1 with CHESS for pharmacological and structural studies

Daniel J. Scott [a,b], Lutz Kummer [a], Pascal Egloff [a], Ross A.D. Bathgate [b], Andreas Plückthun [a,*]

[a] Department of Biochemistry, The University of Zurich, Winterthurerstrasse 190, 8057 Zurich, Switzerland
[b] The Florey Institute of Neuroscience and Mental Health, and The Department of Biochemistry and Molecular Biology, The University of Melbourne, Parkville, Victoria 3010, Australia

ARTICLE INFO

Article history:
Received 26 May 2014
Received in revised form 13 July 2014
Accepted 14 July 2014
Available online 23 July 2014

Keywords:
G protein-coupled receptor
Directed evolution
Stabilization
Encapsulation
Detergent
Thermostability

ABSTRACT

The largest single class of drug targets is the G protein-coupled receptor (GPCR) family. Modern high-throughput methods for drug discovery require working with pure protein, but this has been a challenge for GPCRs, and thus the success of screening campaigns targeting soluble, catalytic protein domains has not yet been realized for GPCRs. Therefore, most GPCR drug screening has been cell-based, whereas the strategy of choice for drug discovery against soluble proteins is HTS using purified proteins coupled to structure-based drug design. While recent developments are increasing the chances of obtaining GPCR crystal structures, the feasibility of screening directly against purified GPCRs in the unbound state (apo-state) remains low. GPCRs exhibit low stability in detergent micelles, especially in the apo-state, over the time periods required for performing large screens. Recent methods for generating detergent-stable GPCRs, however, offer the potential for researchers to manipulate GPCRs almost like soluble enzymes, opening up new avenues for drug discovery. Here we apply cellular high-throughput encapsulation, solubilization and screening (CHESS) to the neurotensin receptor 1 (NTS_1) to generate a variant that is stable in the apo-state when solubilized in detergents. This high stability facilitated the crystal structure determination of this receptor and also allowed us to probe the pharmacology of detergent-solubilized, apo-state NTS_1 using robotic ligand binding assays. NTS_1 is a target for the development of novel antipsychotics, and thus CHESS-stabilized receptors represent exciting tools for drug discovery.

1. Introduction

GPCRs are located in the cell membranes of all human cell types where they serve to detect and transduce extracellular signals into intracellular signaling pathways. The GPCR gene family is the largest in the human genome and encodes approximately 850 different receptors that sense and respond to a huge variety of stimuli including neurotransmitters, metabolites, hormones and environmental stimuli such as light, tastes and smells [1]. This diverse array of stimuli is a testament to the evolutionary success of the protein architecture of GPCRs, made up of seven transmembrane helices, which is maintained throughout the family despite the low sequence homology. Upon activation, GPCRs couple with and stimulate intracellular G-proteins to initiate cellular signaling pathways.

Because of the location of GPCRs on the surface of cells and their involvement in many, if not most, physiological pathways, GPCRs are the major class of drug targets in the human body [2]. Conversely, less than 10% of the GPCR family is currently targeted by prescription drugs [2]. This discrepancy is primarily due to the lack of knowledge about how molecules interact with and activate GPCRs at the molecular level, such that a true molecular design of specific agonists and antagonists has not been possible. Additionally, for a great number of receptors, neither the natural ligand nor the function has been elucidated ("orphan receptors"). Most drugs have thus come from cellular screening of the known receptors.

Modern drug discovery techniques for targeting soluble enzymes, for example, have higher success rates based on improved in vitro screening assays and the parallel application of surface plasmon resonance (SPR) or nuclear magnetic resonance spectroscopy (NMR) based fragment screening, in conjunction with structure-based lead optimization [3]. The hurdle for structural, mechanistic and in vitro drug screening studies of GPCRs is that to apply a similar workflow to GPCRs, the receptors must be solubilized in detergents and purified. However, GPCRs typically exhibit low stability in detergent micelles, especially when a sample is required to be stable in the apo-state for

Abbreviations: GPCR, G protein-coupled receptor; IMP, integral membrane protein; CHESS, cellular high-throughput encapsulation solubilization and screening; NT, neurotensin peptide; FACS, fluorescence-activated cell sorting; EDTA, ethylenediaminetetraacetic acid; DDM, *n*-dodecyl-β-D-maltopyranoside; DM, *n*-decyl-β-D-maltopyranoside; OG, *n*-octyl-β-D-glucopyranoside; CHAPS, 3-[(3-cholamidopropyl)dimethylammonio]-1-propanesulfonate; CHS, cholesteryl hemisuccinate; HTG, *n*-heptyl-β-D-thioglucopyranoside; HTS, high-throughput screening; PBS, phosphate buffered saline; sfGFP, super-folder green fluorescent protein

* Corresponding author at: Biochemisches Institut, Universität Zürich, Winterthurerstr. 190, CH-8057 Zürich, Switzerland. Tel.: +41 44 635 5570; fax: +41 44 635 5712.
E-mail address: plueckthun@bioc.uzh.ch (A. Plückthun).

http://dx.doi.org/10.1016/j.bbamem.2014.07.015
0005-2736/

many hours to facilitate in vitro binding assays and fragment screening using biophysical methods.

Recent progress in obtaining crystal structures of GPCRs [4–19] will undoubtedly aid in the computational optimization of drug leads. Most of these structures were determined as fusion proteins, with T4-lysozyme replacing intracellular loop 3 [5,20], which acts as a rigid scaffold that promotes the formation of crystal contacts in lipidic-cubic phase crystallization trials. The fusion strategy is necessary so that sufficient protein surface area is displayed outside of the lipid bilayer, because for most unmodified GPCRs, virtually all of the protein is embedded within the bilayer and thus unable to contribute to crystal contact formation. This technique does not significantly increase the stability of the receptor in the solubilized state [20,21] and, because the receptors are reconstituted into insoluble media, this strategy is not useful for direct high-throughput screening for interacting molecules. Furthermore, such a fusion disallows interaction between the GPCR and G proteins so that signaling as a readout is not an option.

A pioneering approach to making GPCRs more accessible to structural, biochemical and biophysical methods is to stabilize the receptors by introducing thermostabilizing mutations. Stabilizing mutations have been identified using semi-rational or alanine-scanning and screening approaches [5,22–26], and with directed evolution methods [27–31]. Stabilized GPCRs can be successfully applied to crystallization [7,14,19,32–35], robotic in vitro binding assays in the solubilized form [31], and fragment screening using biophysical methods [36,37]. Generally, these studies require the receptor to be purified in the presence of a ligand to stabilize the receptors during the time needed for purification and assay setup. This necessitates extensive washing to remove bound ligand before assays can be conducted [36], and the instability of these receptors in the apo-state may limit the time that samples can be probed to unrealistically short intervals. To enable reliable measurements of GPCR samples over the time scales required for high-throughput screening (HTS) assays or NMR-based fragment screening, receptors are required that are stable for many hours, preferably in the apo-state. Here we use the cellular high-throughput encapsulation, solubilization and screening (CHESS) method to evolve neurotensin receptor 1 (NTS_1) mutants that meet these requirements. The crystal structure of one of the resultant receptors was recently solved in a detergent-solubilized form [19]. Here we demonstrate that the long-term, apo-state stability of these CHESS-stabilized NTS_1 variants makes them suited to HTS-compatible ligand binding assays using isolated receptors in detergent micelles.

2. Materials and methods

2.1. Stabilization of NTS_1 using CHESS

Escherichia coli strain DH5α was transformed with the StEPM303 library and receptor expression was induced as described previously [29,31]. 1.75×10^{10} cells from the expression culture were encapsulated with one layer of chitosan and 1 layer of alginate as described previously [31]. For the initial selection round, the capsule population was exposed to PBS pH 7.4, 1 mM EDTA and 1.7% DM (termed PBS-E(DM)) for 3 h at 20 °C with vigorous shaking without ligand, followed by 2 h at 20 °C in the presence of 20 nM BODIPY FL-labeled NT(8–13) (FL-NT). Capsules were washed twice in PBS-E(DM) and subjected to FACS using a FACSAria III cell sorter (BD Biosciences). Capsules exhibiting the top 0.5–1% of fluorescence of the population were retained, resulting in the collection of 50,000 capsules. Genetic information was recovered from sorted capsules by PCR amplification using NTS_1-specific primers after incubation in an ultrasonic water bath for 5 min. For the second round of selection, the amplified receptor genes were re-cloned, proteins expressed and the cells encapsulated as above. The capsule population was first treated with PBS-E(DM) for 3 h at 20 °C, followed by addition of 20 nM FL-NT for 1 h at 20 °C, before the capsules were collected by centrifugation and resuspended in PBS-E containing 2% octyl-β-D-glucopyranoside (OG) (PBS-E(OG)) and 20 nM FL-NT at 4 °C. Capsules were washed once in 20 nM FL-NT in PBS-E(OG) to promote efficient detergent exchange before being incubated for 2 h in PBS-E(OG) with ligand at 4 °C. Capsules were washed twice in PBS-E(OG) and subjected to FACS as above, resulting in the collection of 38,000 capsules. These clones were isolated and re-cloned as above for a third round of selection. In the third round of selection, the capsules were exposed to PBS-E(DM) for 3 h at 20 °C, followed by the addition of 20 nM FL-NT for 1 h at 20 °C, before the capsules were collected by centrifugation and resuspended in PBS-E containing 2% heptyl-β-D-thioglucopyranoside (HTG) (PBS-E(HTG)) and 20 nM FL-NT at 4 °C. Capsules were washed once in 20 nM FL-NT in PBS-E(HTG) to promote efficient detergent exchange before being incubated for 25 h at 4 °C. After this step, capsules were washed twice in PBS-E(HTG) and sorted with FACS as above, resulting in the collection of 20,000 capsules. The DNA encoding these clones was isolated and re-cloned into an expression vector containing a C-terminal sfGFP fusion, as in [31]. The CHESS workflow is depicted in Fig. 1.

2.2. Stability analysis of 96 individual NTS_1 variants from the selected population

Forty-seven individual colonies derived from the capsules sorted in the 3rd round of CHESS (Section 2.2) were picked and used to inoculate 1.2 ml cultures of LB broth containing 100 μg/ml ampicillin and 1% glucose in a 96-deep-well plate. As a control, a colony of cells transformed with a previously stabilized NTS_1 variant (C7E02) [29] was also picked. Cultures were grown for 16 h at 37 °C before being used to inoculate 48, 5-ml-expression cultures in 24-deep-well plates. Receptors were expressed as described previously at 20 °C for 20 h [31]. The initial cultures were centrifuged and the plasmid DNA isolated. After expression, cell pellets were solubilized in 1 ml PBS-E(DM) for 2 h at 20 °C and the cell debris pelleted with centrifugation at 5000 *g* for 20 min. 0.8 ml of the supernatant was transferred to a 96-well KingFisher plate (Thermo Scientific) containing 20 μg of streptavidin T1 Dynabeads (Life Technologies) per well. Samples were then robotically manipulated using a KingFisher Flex robot (Thermo Scientific) as described previously [31], including binding of 20 nM HL-NT for 1 h, exchanging the detergent to 2% HTG for 1.5 h, washing away unbound ligand for 5 min and eluting the beads into 0.25 ml PBS-E(HTG) for the analysis of ligand binding in a fluorescent plate reader (Tecan M1000) and with flow cytometry (Partec CyFlow Space). 100,000 beads from the binding assay were measured with flow cytometry, with the average fluorescence intensity of single-sized beads presented in Fig. 2B upon 638 nm laser excitation and emission at 675 nm (20 nm bandpass).

2.3. Construct optimization

Based on the stability screen, the most promising stabilized variant, number 47 (termed NTS_1-H4) was sequenced. Before further analysis with fluorescent binding assays, the following changes were made to the receptor. A mutation in the conserved E/DRY motif was reverted (L167R), a potential human rhinovirus 3C protease site was removed from intracellular loop 3 (Q274A), alanine 342 in extracellular loop 3 was reverted to the naturally occurring phenylalanine (A342F) and all exposed cysteines were mutated to either alanine or serine (C278A, C386A, C388A, C417S) for allowing the future introduction of unique cysteines. The resultant receptor was termed NTS_1-H4(BM1) and the encoding gene was synthesized by Genscript.

2.4. Stability comparison of engineered NTS_1 variants

Stability measurements of selected NTS1 receptor variants were performed as described previously [28,31]. NTS1 receptor variants were expressed with a C-terminal sfGFP-Avi-tag fusion. A cell pellet corresponding to a 2.5 ml expression culture was used for one single measurement reporting functionally folded receptor as determined by a ligand binding assay. Receptors were solubilized in solubilization

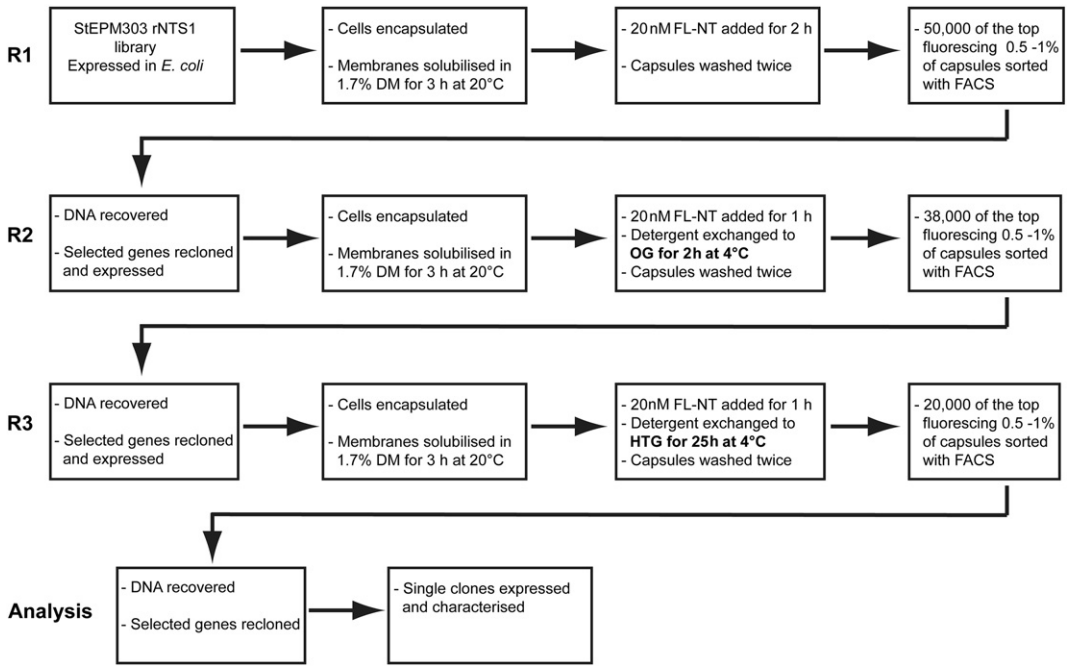

Fig. 1. CHESS-based selection workflow for generating NTS_1 mutants that were resistant to short-chain detergents, apo-state solubilization and long term incubations in the solubilized state. CHESS rounds are indicated by R1-3. For a diagrammatic representation of the CHESS method, see Scott and Plückthun [31].

buffer (PBS pH 7.4, 1% (w/v) DDM, 0.5% (w/v) CHAPS, 0.1% (w/v) CHS, 1 mM EDTA, complete protease inhibitors (Roche), 40 μg/ml deoxyribonuclease I (Roche), 1 mg/ml lysozyme). Solubilization was performed at 4 °C for 2 h. Cell debris was removed by centrifugation and the supernatant was exposed to streptavidin-coated paramagnetic beads. Solubilized receptor variants were allowed to bind to the beads for 1 h at 4 °C before being transferred in 96-well plates for subsequent manipulation with a KingFisher Flex magnetic particle processor. Receptor-coated beads were subjected to detergent solution, PBS-E(DCC) (PBS pH 7.4, 1 mM EDTA, 1% (w/v) DDM, 0.5% (w/v) CHAPS, 0.1% (w/v) CHS) with or without 20 nM Hilyte-647 labeled neurotensin 8–13 (HL647-NT). Non-specific binding was determined by adding

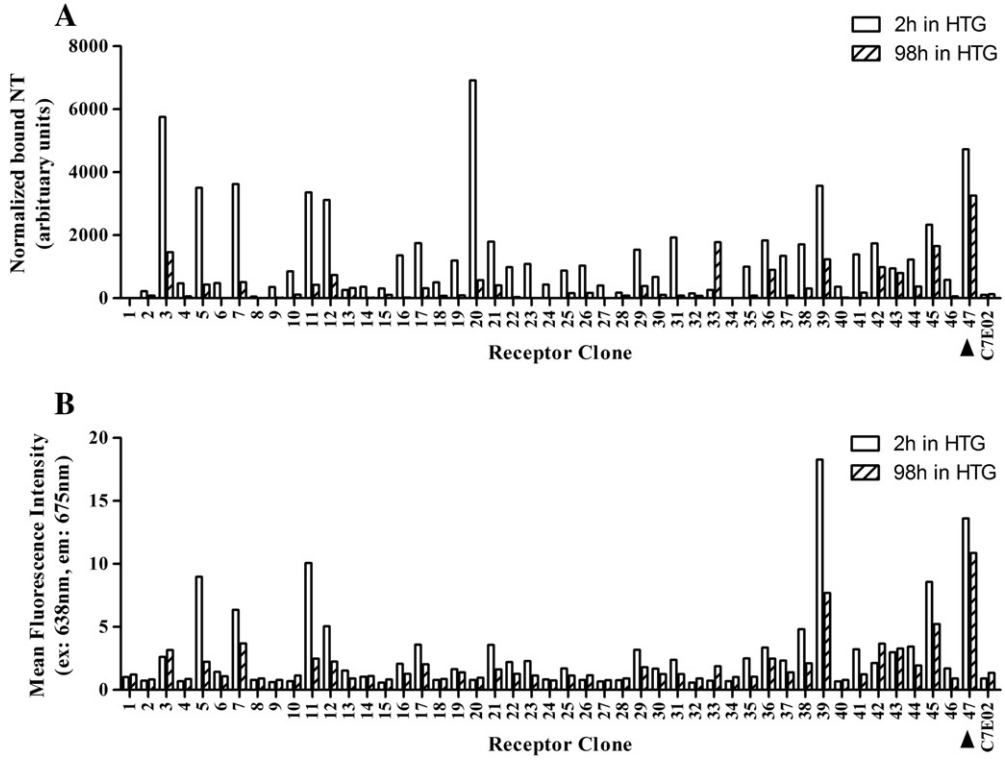

Fig. 2. Single-clone analysis of 47 selected NTS_1 mutants after 3 rounds of CHESS. Detergent-solubilized, biotinylated receptors were captured onto streptavidin-coated magnetic beads. The ability of the receptor-coated beads to specifically bind HL-NT after 2 h (open columns) or 98 h (striped columns) in the short-chain detergent HTG was measured using a fluorescent plate reader (A), or an analytical cytometer (B). Clone 47, indicated with arrows, was termed NTS_1-H4.

excess (1 μM) unlabeled NT8-13 competitor to the binding solutions. After a further 0 h or 18 h exposure to DDM, beads were washed twice with PBS-E(DCC) and those exposed to detergent in the unbound state were transferred to solutions containing 20 nM HL647-NT with or without competitor for 1.5 h. Receptor-coated beads were washed twice in PBS-E(DCC) and transferred to black 96-well microplates (Greiner) in a final volume of 100 μl. HL647-NT and sfGFP fluorescence levels were measured in each well using an M1000 dual monochromator fluorescence plate reader (Tecan) with excitation at 630 nm for HL647-NT and 488 nm for sfGFP. Fluorescence emission for HL647-NT was measured at 680 nm and for sfGFP at 530 nm.

Thermal stability measurements in PBS-E(DCC) of NTS1 receptor variants were essentially performed as described for the analysis of detergent stability (see above). After exposure of solubilized receptor variants to streptavidin-coated paramagnetic beads, receptor-coated beads were resuspended in PBS-E(DCC) with or without ligand (or competitor). Beads were transferred to 96-well PCR plates and exposed to different temperatures for 30 min in a gradient PCR cycler (Biometra). After heat treatment, receptor-coated beads that were heated in the absence of ligand were incubated with PBS-E(DCC) containing 20 nM HL647-NT or competitor for 1.5 h. Beads were washed twice in PBS-E(DCC) and transferred to black 96-well microplates and fluorescence intensities of HL647-NT and sfGFP in each well were determined as above. The data were analyzed by nonlinear regression fitting with GraphPad Prism.

2.5. KingFisher saturation binding assays

NTS_1-H4(BM1) was expressed in 400 ml cultures for 20–24 h at 20 °C, the cells harvested with centrifugation and the pellet resuspended in 10 ml 50 mM HEPES (pH 7.8) containing 200 mM NaCl, 10 mM EDTA, 1 mg/ml chicken lysozyme, 10 U/ml DNAse, 1.7% DM and 0.5% CHAPS. Cells were solubilized at 20 °C with vigorous shaking for 3 h. Cell debris was removed with centrifugation at 15,000 *g* for 10 min at 4 °C. The supernatant containing solubilized receptor was then incubated with streptavidin-coated paramagnetic beads, 2.5 μg of beads per ml of culture, at 4 °C for 1 h to immobilize the biotinylated receptor onto the beads. Beads were collected with centrifugation at 5,000 *g* for 5 min and resuspended in assay buffer (50 mM HEPES (pH 7.8), 200 mM NaCl, 10 mM EDTA and 0.1% DM) at a final concentration of 100 μg beads per ml. 20 μg of beads were then added to 48 wells of a deep well KingFisher plate (plate #1) (Thermo Scientific). A concentration series of Alexa-647 labeled neurotensin 8–13 (A647-NT) was made in assay buffer and 1 ml of each added to several wells of a separate KingFisher plate (plate #2). For each A647-NT concentration, a separate solution was made containing an excess of unlabeled neurotensin 8–13 (10 μM), with 1 ml of each being aliquoted into designated wells of plate #2. 200 μl and 100 μl of assay buffer were added to 48 wells of another two KingFisher plates, plate #3 and plate #4 respectively. A KingFisher 96 magnetic particle processor was used to automatically perform the following steps at 4 °C: the beads were captured from plate #1 and transferred to plate #2, beads and ligand solutions were mixed for 2 h at 4 °C, and beads were transferred to plate #3 and washed for 1.5 min before being transferred to plate #4. Beads were transferred with a multichannel pipette from KingFisher plate 4 to a Greiner non-binding black 96-well plate. The sfGFP (excitation filter 485 nm, band pass 12 nm, emission filter 520 nm, band pass 10 nm) and Alexa-647 (excitation filter 640 nm, band pass 10 nm, emission filter 670 nm, band pass 10 nm) signals from each well were measured using an Omega Polarstar plate reader (BMG Labtech). To determine if ligand depletion was occurring during the binding incubation, 50 μl of the A647-NT solutions in KingFisher plate #2 was transferred to a Greiner non-binding fluorescence 96-well plate and the Alexa-647 signals of the wells compared. Data were analyzed with GraphPad Prism, with curves fitted using the one site — total and nonspecific binding equations.

2.6. KingFisher competition binding assays

Receptor-coated bead samples were prepared and aliquoted into KingFisher plate #1 as described in Section 2.5. In plate #2, concentration series of the various competitors were added, all in assay buffer supplemented with 2 nM A647-NT, 0.5 ml per well. Competitors included SR 48692 (Tocris Biosciences and Sigma Aldrich), SR 142948 (Tocris Biosciences), neurotensin 8–13 (Sigma Aldrich) and neurotensin 1–12 (synthesized by GL Biochem, Shanghai, China). The binding assays were performed using a KingFisher 96 robot and Omega Polarstar plate reader as in Section 2.5. Data were analyzed using GraphPad Prism with curves fitted using the one site — fit Ki equation. Data from 3 separate experiments were pooled and the estimated K_d values for A647-NT calculated in Section 2.5 were used to fit the competition curves.

3. Results

3.1. CHESS based evolution of apo-state stable NTS_1 variants

To evolve an NTS_1 variant that could be purified in short-chain detergents for X-ray crystallization and exhibit apo-state and long-term stability in the solubilized form, we used the highly diverse StEPM303 library of NTS_1 mutants and selected using CHESS, following the strategy outlined in Fig. 1. In each selection round, the encapsulated GPCRs were solubilized for 3 h, at 20 °C, in the absence of ligand to place selective pressure on apo-state stability. In the second and third rounds of selection, the encapsulated receptor population was exposed to the short-chain detergents OG and HTG, respectively, placing selective pressure on the population for stability in detergents that are suitable for vapor diffusion crystallization of GPCRs. Finally, the long-term stability was selected for by leaving the third generation of the evolving population of GPCRs in HTG for 25 h before selecting out the most stable clones with FACS.

3.2. Isolating NTS_1-H4 from the CHESS selected population

The genes encoding the CHESS-selected NTS_1 variants were isolated from the sorted capsules and cloned into an expression vector comprising C-terminal sfGFP and avi-tag (for in vivo biotinylation) fusions. Unlike GFP, sfGFP folds rapidly into a highly stable fluorescent protein that does not act as a folding reporter, but rather as a measure of total protein concentration [38]. The stability of 47 receptor variants was assayed by testing their ability to bind a fluorescently labeled neurotensin ligand after solubilization in HTG for 2 h and 98 h (Fig. 2). In this assay, solubilized receptors were captured on streptavidin-coated beads and exposed to fluorescently labeled neurotensin 8–13 (HL-NT). The ability of each clone to bind ligand at the given time points was determined by washing the beads and measuring the amount of HL-NT bound to the beads with a fluorescent plate reader (Fig. 2A) and a flow cytometer (Fig. 2B). Of these receptors, clone 47 (NTS_1-H4) was selected for further analysis because of its ability to bind high levels of NT after 2 h and 98 h solubilized in HTG, when measured with both methods.

3.3. Comparison of the stability of NTS_1-H4 to other NTS_1 variants

To determine whether NTS_1-H4 exhibited favorable long-term and apo-state stability, we compared the stability of this receptor to three other variants: (i) wild-type rat NTS_1, (ii) a thermostabilized variant produced through systematic mutation by Shibata et al. [26] (NTS_1-7m), and (iii) a highly optimized variant generated through evolution using bacterial display and systematic mutation by Schlinkmann et al. (TM86V) [29,31]. Each receptor was expressed in *E. coli* with an sfGFP-avi-tag C-terminal fusion, resulting in the production of fluorescent, biotinylated receptor. Unmodified NTS_1 is not stable in detergents such

as DM, OG and HTG, so to enable comparison across the receptor variants, we solubilized the cells in a mild detergent mix (PBS-E(DCC)). Solubilized receptors were immobilized on streptavidin-coated beads and subjected to a range of temperatures for 30 min in the presence (Fig. 3A) or absence (Fig. 3B) of fluorescently labeled neurotensin to generate thermostability curves. Such curves are commonly used to rank the stabilities of engineered GPCRs, and the temperature at which only half the receptor proteins are able to bind ligand is referred to as the apparent melting temperature (T_m). NTS_1-H4 exhibited the highest thermostability of all the variants when heated in both the presence ($T_m = 57$ °C) and absence ($T_m = 48.1$ °C) of excess neurotensin (Fig. 3A–B). Thus, the thermostability of NTS_1-H4 in this harsh detergent is improved by 21.6 °C in the bound state and 26.8 °C in the apo-state compared to unmodified NTS_1.

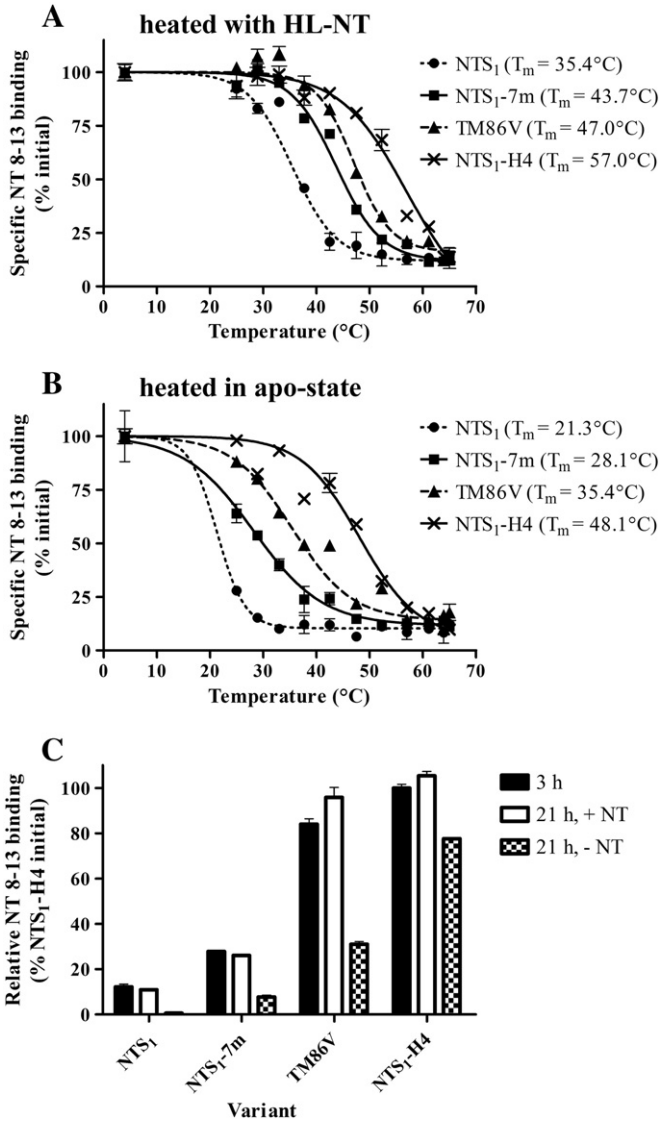

Fig. 3. The stabilities of thermostabilized NTS_1 mutants generated using different methods were compared to wild type NTS_1. The thermostabilities of wild-type rat NTS_1 (NTS_1, filled circles with dotted lines), NTS_1-7m (filled squares with solid lines), TM86V (filled triangles with dashed lines) and NTS_1-H4 (crosses with solid lines) were measured with the receptors heated in the presence of HL-NT (A) or in the apo-state (B). To allow WT to be analyzed as well, the experiment was carried out in DDM/CHAPS/CHS. Apparent melting temperatures (T_m) were determined with non-linear regression and are displayed in parentheses next to the figure keys. (C) Long-term stability of the 4 receptors was assayed by measuring the relative levels of HL-NT binding 3 h after solubilization (filled columns), 21 h after solubilization, and 18 h of which the receptors were incubated with HL-NT (open columns), or 21 h after solubilization incubated in the apo-state (checkered columns). The receptors were incubated at 4 °C.

The relative amount of folded receptor in each of the samples was monitored after 3 h in the apo-state and either 21 h in the apo-state or with HL-NT bound at 4 °C. The relative levels of folded receptor were calculated by measuring the ratio of bound HL-NT fluorescence (level of folded protein) to the sfGFP fluorescence (total protein) in each sample at various time points. As expected, unmodified NTS_1 displayed the lowest level of folded receptor under each condition, closely followed by NTS_1-7m (Fig. 3C). Interestingly, for all the receptor samples, there was no significant difference in the relative NT binding levels after a 21 h incubation at 4 °C in the presence of HL-NT. There was a striking difference, however, when the solubilized receptors were incubated for 21 h at 4 °C in the absence of NT (Fig. 3C). Under these conditions, no binding of NT could be detected on NTS_1, while NT binding to NTS_1-7m and TM86V was decreased by 72% and 63% respectively, whereas only a 22% decrease in ligand binding was seen for NTS_1-H4.

3.4. Saturation binding of NT to solubilized NTS_1-H4

The high stability exhibited by NTS_1-H4 in the apo-state indicated that this variant could be used to probe the binding of ligands to solubilized, isolated receptor preparations in a low-cost high-throughput compatible way. To demonstrate this, we expressed and captured NTS_1-H4-sfGFP onto magnetic beads and using a KingFisher magnetic particle processor and fluorescent plate reader, conducted saturation binding assays using Alexa647-NT (Fig. 4A). The ligand binding step was conducted for 2 h at 4 °C in 1 ml of solution, which resulted in no significant ligand depletion, even at only 100 pM A647-NT (Fig. 4B). Non-specific binding was determined by measuring the binding of increasing concentrations of A647-NT in the presence of 1 μM unlabeled NT8-13. To control for differences in bead loading, sfGFP fluorescence was measured in each well and the specific binding was calculated as a ratio of A647-NT fluorescence to sfGFP fluorescence. Fitting the resultant data enabled us to estimate the K_d of A647-NT binding to NTS_1-H4 at 0.65 ± 0.13 nM.

3.5. Competition binding assays using solubilized NTS_1-H4

To probe the binding of unlabeled ligands to solubilized NTS_1-H4, competition binding assays were performed in the same robotic manner, using 2 nM A647-NT as the labeled ligand (Fig. 4C). Unlabeled agonists neurotensin 8–13 (NT8-13) and neurotensin 1–12 (NT1-12), along with antagonists, SR48692 and SR142948, were allowed to compete with A647-NT in a dose-dependent manner (Fig. 4C). Using the estimated K_d value for A647-NT (Section 3.4), from the competition binding experiments we were able to fit K_i values for NT8-13, NT1-12, SR48692 and SR142948, respectively (Table 1).

3.6. Sequence of NTS_1-H4

NTS_1-H4 was sequenced and found to contain 25 amino acid substitutions over wild-type rat NTS_1 including; S83G, A86L, T101R, H103D, H105Y, L119F, M121L, E124D, R143K, D150E, A161V, R167L, R213L, V234L, K235R, V240L, I253A, I260A, N262R, K263R, H305R, C332V, T354S, F358V, and S362A. Of these, H103D, H105Y, A161V, R213L, V234L, H305R and S362A are derived from the parental receptor in the StEPM303 library (NTS_1–DO3) and thus the other 18 mutations were acquired during the selection outlined in Fig. 1. Fig. 5 indicates the positions of these mutations on the crystal structure of NTS_1-H4 [19].

4. Discussion

The critical advantage of CHESS over other techniques is that millions of GPCR-mutant-containing microcapsules can be screened directly for the desired stability properties within an hour by using FACS.

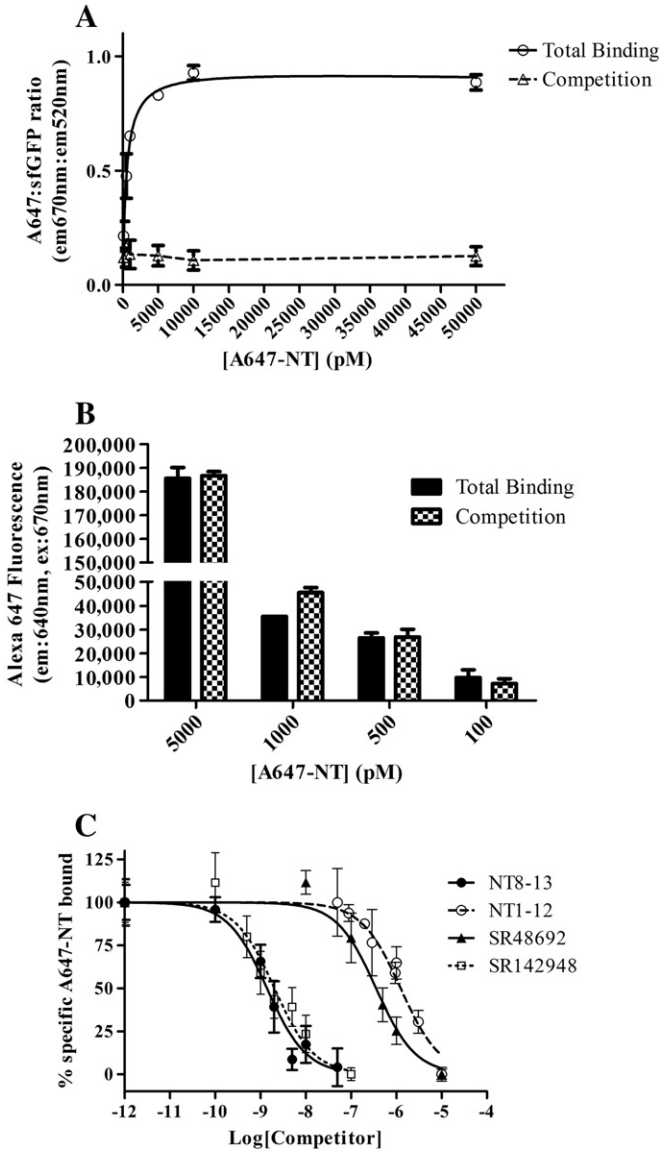

Fig. 4. Saturation (A–B) and competition (C) binding assays were performed on solubilized, biotinylated and sfGFP tagged NTS_1-H4, immobilized on streptavidin-coated magnetic beads. For saturation binding (A), beads were exposed to increasing concentrations of A647-NT in the presence of excess NT8-13 (COMPETITION, open triangles, dashed line) or without competition (TOTAL BINDING, open circles, solid line). The ratio of A647-NT to sfGFP fluorescence was measured to account for slight differences in bead concentrations across the 96-well plates. (B) Potential ligand depletion was assayed by measuring the levels of A647-NT retained in the binding wells from (A) upon the removal of the receptor-coated beads. A decrease in A647-NT in the total binding wells (black columns) compared to the competition wells (checkered columns), where unlabeled NT would saturate the receptor and thus no ligand can be removed, would indicate depletion of A647-NT in the binding step. No ligand depletion was observed. For competition binding (C), NTS_1-H4 coated beads were exposed to 2 nM A647-NT and increasing concentrations of unlabeled NT8-13 (filled circles with solid line), NT1-12 (open circle with dashed line), SR48692 (filled triangles and solid line) and SR142948 (open squares with dotted line). The ratio of A647-NT to sfGFP fluorescence was measured, with the data sets normalized to 100% based on the fluorescence of wells containing no competitor. Mean values ± the standard error of the mean (SEM) are plotted from data pooled across 3 separate experiments.

Here we panned the StEPM303 library [29] for NTS_1 mutants that were stable in short-chain detergents that are desirable for crystallization. In addition, we selected for stability over 24 h in such detergents, as well as receptors that are exhibiting apo-state stability. We believe such properties to be highly desirable for the application of the experimental methods commonly used for structure-based drug design.

Table 1
Binding constants derived from competition binding experiments using solubilized NTS_1-H4.

Ligand	Fitted constant	nM	SEM	Figure
NT8-13	K_i	0.34	0.09	Fig. 4C
NT1-12	K_i	306	77	Fig. 4C
SR48692	K_i	87	27	Fig. 4C
SR142948	K_i	0.5	0.1	Fig. 4C

The encapsulated cells were resistant to HTG over these time periods, and genes encoding highly stable NTS_1 mutants could be isolated from the sorted capsules that exhibited high fluorescent ligand binding (Fig. 2). The clone that was able to bind the most fluorescent ligand after 2 h and 98 h solubilized in HTG, when measured using 2 different instruments, was termed NTS_1-H4. NTS_1-H4 exhibited all of the properties we were seeking, including high thermostability when heated in the presence and absence of ligand (Fig. 3A–B), and long-term, apo-state stability in detergent (Fig. 3C).

Because NTS_1 has been stabilized using several methods, we were able to directly compare the resultant receptors with the wild-type protein. NTS_1-7m was stabilized using the systematic mutagenesis approach [26] and TM86V was derived through a combination of evolution with bacterial display for high expression and systematic mutagenesis [29]. Using a detergent mixture known to maintain unmodified $rNTS_1$ in a stable state under mild conditions [39,40], thermostability assays were performed on the 4 receptors (Fig. 3A-B). When heated in both the presence and absence of ligand, NTS_1-H4 was the most thermostable, followed by TM86V, NTS_1-7m and wild type. Compared to $rNTS_1$, NTS_1-H4 exhibited 21.6 °C and 26.8 °C improvement in thermostability when heated in the bound and apo-state respectively, the most stable by over 10 °C. NTS_1-H4 also exhibited the highest stability of the 4 receptors when incubated in detergent for over 21 h in the presence or absence of bound ligand (Fig. 3C).

This high level of apo-state stability meant that we could successfully use bacterially expressed NTS_1-H4, captured onto magnetic beads, in robotic fluorescence-based saturation and competition binding assays (Fig. 4). From fitting the saturation binding curves the K_d of the fluorescently labeled neurotensin analogue, Alexa-647-labeled neurotensin 8–13 (A647-NT), could be estimated to be 0.65 nM ± 0.13, which compares well to K_i values reported for unlabeled versions of this peptide using NTS_1 expressing cells and tissues [41]. The high signal-to-noise ratio in the saturation binding assays using this labeled peptide enabled us to conduct competition binding assays using a sub-saturating concentration of A647-NT (2 nM). K_i values for the binding of unlabeled NT8-13, NT1-12, SR48692 and SR142948 to NTS_1-H4 were calculated from the resultant curves (Fig. 4C and Table 1). Calculated K_i values compared well to the literature values for NT8-13 [41], NT1-12 [42] and SR142948 [43], where cell culture and tissue preparations were used for NTS_1 competition binding assays. This demonstrated that our engineered, bacterially expressed and detergent-solubilized GPCR exhibited native-like ligand binding behavior.

Interestingly, the antagonist SR48692 was less potent at competing A647-NT binding to solubilized NTS_1-H4, compared to WT NTS_1 (which could only be tested in cell-based binding studies), by a factor between 2.7 and 44 fold, depending on the values cited in the literature [43–45]. The affinity of SR48692 to the thermostabilized NTS_1 variant NTS_1-GW5 was reduced even by 130–200 fold when measured in insect cell membranes, whereas binding of the agonist to this receptor was unaltered [14]. This points to a mutation that may reduce antagonist affinity compared to agonist affinity, even though a small influence of solubilization cannot be excluded.

NTS_1-H4 and NTS_1-GW5 share only one homologous stabilizing mutation at position 358 in TM7, which is a substitution from Phe to Ala in NTS_1-GW5 and to Val in NTS_1-H4. Mutation of this position to alanine has been reported to reduce the affinity of SR48692 for NTS_1 but not that of neurotensin [45] and result in a constitutively active receptor

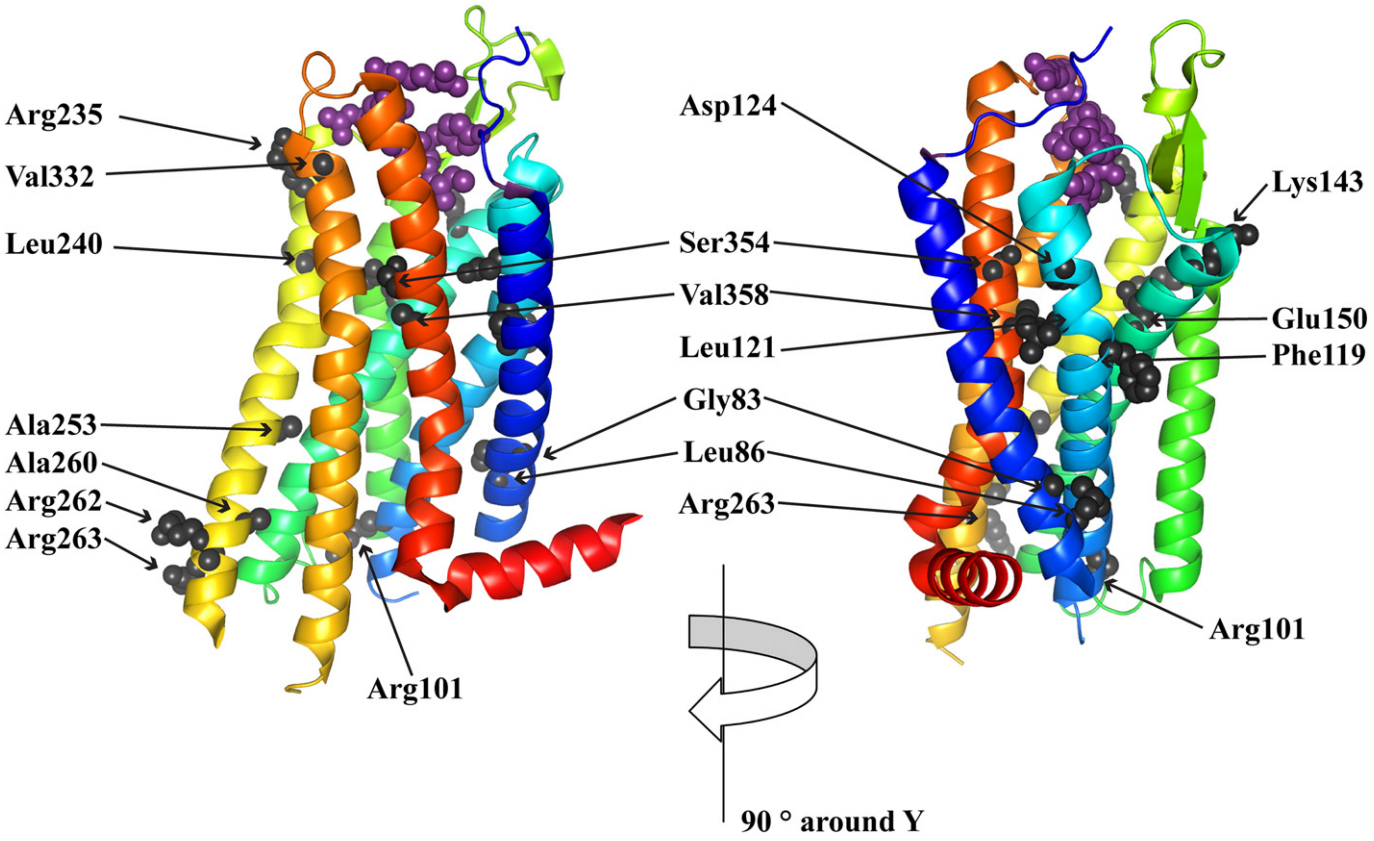

Fig. 5. Positions of CHESS-selected mutations in the crystal structure of NTS_1-H4 (PDB ID: 4BWB) displayed at two angles rotated by 90°. TM1 is colored dark blue, TM2 light blue, TM3 cyan, TM4 green, TM5 yellow, TM6 orange,TM7 red and neurotensin purple.

with respect to inositol phosphate production [46], suggesting that the lower affinity of SR48692 for both NTS_1-H4 and NTS_1-GW5 may be a result of the mutation at position 358. Overall, engineering NTS_1-H4 to be detergent-stable in the apo-state has enabled us to pharmacologically characterize the orthosteric binding site of a detergent-solubilized GPCR using low cost, high-throughput compatible assays.

Thermostabilization of NTS_1 has so far resulted in the determination of 5 structures of different receptor variants or constructs. NTS_1-GW5 was engineered using systematic mutagenesis [47], and the crystal structure of this receptor, produced in insect cells, was determined using the T4-lysozyme fusion and lipidic cubic phase crystallization approach [14]. The crystal structures of two NTS_1–TM86V constructs, derived from directed evolution using bacterial display [29], were recently solved in detergent using vapor diffusion crystallization [19] without any fusion to another protein. In the same study, the structures of two more receptors were determined, NTS_1-G7 [31] and NTS_1-H4 (engineered in this manuscript), which were stabilized using CHESS. Of note is that the structures of NTS_1–TM86V, NTS_1-G7 and NTS_1-H4 were the first GPCR structures solved from bacterially expressed protein. Furthermore, the direct selection of NTS_1-G7 and NTS_1-H4 for stability in short-chain detergents allowed these receptors to be crystallized in short-chain detergents using vapor diffusion crystallography without any systematic mutational optimization.

A thorough comparison of the 5 structures can be found in Egloff et al. [19]. While NTS_1-H4 is the most thermostable variant described to date, it also contains the most mutations. In Fig. 5, the CHESS selected mutations in NTS_1-H4 are highlighted in the crystal structure. Selected mutations were relatively evenly distributed across transmembrane domains (TMs) 1–3 and TMs 5–7, with the most mutations occurring in TM5 (6 substitutions) (Fig. 5). NTS_1-7m, NTS_1-GW5, TM86V, NTS_1-G7 and NTS_1-H4 only share homologous stabilizing mutations at positions 86 (A86L) and 358 (F358A or V), indicating that stabilization can be achieved through a variety of mutational modes.

In addition to structure determination, purified thermostabilized GPCRs have also proven to be useful tools for biophysical analysis of ligand binding and fragment screening [36,37,48]. For these types of studies it is highly beneficial to have apo-receptor samples that are stable in detergents over the long time periods needed to measure binding kinetics, and that will not denature upon ligand dissociation. The engineering of NTS_1-H4 is a demonstration of the utility of CHESS for evolving receptors with the properties needed to conduct biochemical and biophysical experiments on solubilized, purified GPCRs.

Acknowledgements

We acknowledge the professional help given by the staff of the Center for Microscopy and Image Analysis at the University of Zurich, where all FACS was performed, particularly Vinko Tosevski and Claudia Dumrese. Natasha Lam, The Florey Institute, is acknowledged for her assistance in conducting the saturation and competition binding assays. This work was supported by a C. J. Martin Biomedical Overseas Fellowship (520309) from the National Health and Medical Research Council of Australia and a postdoctoral fellowship from the Forschungskredit of the University of Zurich (both to D.J.S.). This project was funded by the Swiss National Science Foundation NCCR Structural Biology 51NF40-117226 and subsequent grant 31003A_153143 (both to AP).

References

[1] R. Fredriksson, H.B. Schiöth, The repertoire of G-protein-coupled receptors in fully sequenced genomes, Mol. Pharmacol. 67 (2005) 1414–1425.
[2] J.P. Overington, B. Al-Lazikani, A.L. Hopkins, How many drug targets are there? Nat. Rev. Drug Discov. 5 (2006) 993–996.

[3] J.S. Mason, A. Bortolato, M. Congreve, F.H. Marshall, New insights from structural biology into the druggability of G protein-coupled receptors, Trends Pharmacol. Sci. 33 (2012) 249–260.
[4] K. Palczewski, T. Kumasaka, T. Hori, C.A. Behnke, H. Motoshima, B.A. Fox, I. Le Trong, D.C. Teller, T. Okada, R.E. Stenkamp, M. Yamamoto, M. Miyano, Crystal structure of rhodopsin: a G protein-coupled receptor, Science 289 (2000) 739–745.
[5] V. Cherezov, D.M. Rosenbaum, M.A. Hanson, S.G. Rasmussen, F.S. Thian, T.S. Kobilka, H.J. Choi, P. Kuhn, W.I. Weis, B.K. Kobilka, R.C. Stevens, High-resolution crystal structure of an engineered human beta2-adrenergic G protein-coupled receptor, Science 318 (2007) 1258–1265.
[6] V.P. Jaakola, M.T. Griffith, M.A. Hanson, V. Cherezov, E.Y. Chien, J.R. Lane, A.P. Ijzerman, R.C. Stevens, The 2.6 Ångström crystal structure of a human A2A adenosine receptor bound to an antagonist, Science 322 (2008) 1211–1217.
[7] T. Warne, M.J. Serrano-Vega, J.G. Baker, R. Moukhametzianov, P.C. Edwards, R. Henderson, A.G. Leslie, C.G. Tate, G.F. Schertler, Structure of a beta1-adrenergic G-protein-coupled receptor, Nature 454 (2008) 486–491.
[8] E.Y. Chien, W. Liu, Q. Zhao, V. Katritch, G.W. Han, M.A. Hanson, L. Shi, A.H. Newman, J.A. Javitch, V. Cherezov, R.C. Stevens, Structure of the human dopamine D3 receptor in complex with a D2/D3 selective antagonist, Science 330 (2010) 1091–1095.
[9] B. Wu, E.Y. Chien, C.D. Mol, G. Fenalti, W. Liu, V. Katritch, R. Abagyan, A. Brooun, P. Wells, F.C. Bi, D.J. Hamel, P. Kuhn, T.M. Handel, V. Cherezov, R.C. Stevens, Structures of the CXCR4 chemokine GPCR with small-molecule and cyclic peptide antagonists, Science 330 (2010) 1066–1071.
[10] T. Shimamura, M. Shiroishi, S. Weyand, H. Tsujimoto, G. Winter, V. Katritch, R. Abagyan, V. Cherezov, W. Liu, G.W. Han, T. Kobayashi, R.C. Stevens, S. Iwata, Structure of the human histamine H1 receptor complex with doxepin, Nature 475 (2011) 65–70.
[11] K. Haga, A.C. Kruse, H. Asada, T. Yurugi-Kobayashi, M. Shiroishi, C. Zhang, W.I. Weis, T. Okada, B.K. Kobilka, T. Haga, T. Kobayashi, Structure of the human M2 muscarinic acetylcholine receptor bound to an antagonist, Nature 482 (2012) 547–551.
[12] M.A. Hanson, C.B. Roth, E. Jo, M.T. Griffith, F.L. Scott, G. Reinhart, H. Desale, B. Clemons, S.M. Cahalan, S.C. Schuerer, M.G. Sanna, G.W. Han, P. Kuhn, H. Rosen, R. C. Stevens, Crystal structure of a lipid G protein-coupled receptor, Science 335 (2012) 851–855.
[13] A. Manglik, A.C. Kruse, T.S. Kobilka, F.S. Thian, J.M. Mathiesen, R.K. Sunahara, L. Pardo, W.I. Weis, B.K. Kobilka, S. Granier, Crystal structure of the mu-opioid receptor bound to a morphinan antagonist, Nature 485 (2012) 321–326.
[14] J.F. White, N. Noinaj, Y. Shibata, J. Love, B. Kloss, F. Xu, J. Gvozdenovic-Jeremic, P. Shah, J. Shiloach, C.G. Tate, R. Grisshammer, Structure of the agonist-bound neurotensin receptor, Nature 490 (2012) 508–513.
[15] H. Wu, D. Wacker, M. Mileni, V. Katritch, G.W. Han, E. Vardy, W. Liu, A.A. Thompson, X.P. Huang, F.I. Carroll, S.W. Mascarella, R.B. Westkaemper, P.D. Mosier, B.L. Roth, V. Cherezov, R.C. Stevens, Structure of the human kappa-opioid receptor in complex with JDTic, Nature 485 (2012) 327–332.
[16] C. Zhang, Y. Srinivasan, D.H. Arlow, J.J. Fung, D. Palmer, Y. Zheng, H.F. Green, A. Pandey, R.O. Dror, D.E. Shaw, W.I. Weis, S.R. Coughlin, B.K. Kobilka, High-resolution crystal structure of human protease-activated receptor 1, Nature 492 (2012) 387–392.
[17] K. Hollenstein, J. Kean, A. Bortolato, R.K. Cheng, A.S. Dore, A. Jazayeri, R.M. Cooke, M. Weir, F.H. Marshall, Structure of class B GPCR corticotropin-releasing factor receptor 1, Nature 499 (2013) 438–443.
[18] F.Y. Siu, M. He, C. de Graaf, G.W. Han, D. Yang, Z. Zhang, C. Zhou, Q. Xu, D. Wacker, J.S. Joseph, W. Liu, J. Lau, V. Cherezov, V. Katritch, M.W. Wang, R.C. Stevens, Structure of the human glucagon class B G-protein-coupled receptor, Nature 499 (2013) 444–449.
[19] P. Egloff, M. Hillenbrand, C. Klenk, A. Batyuk, P. Heine, S. Balada, K. Schlinkmann, D.J. Scott, M. Schütz, A. Plückthun, Structure of signaling-competent neurotensin receptor 1 obtained by directed evolution in *E. coli*, Proc. Natl. Acad. Sci. U. S. A. 111 (2014) E655–E662.
[20] E. Chun, A.A. Thompson, W. Liu, C.B. Roth, M.T. Griffith, V. Katritch, J. Kunken, F. Xu, V. Cherezov, M.A. Hanson, R.C. Stevens, Fusion partner toolchest for the stabilization and crystallization of G protein-coupled receptors, Structure 20 (2012) 967–976.
[21] D.M. Rosenbaum, V. Cherezov, M.A. Hanson, S.G. Rasmussen, F.S. Thian, T.S. Kobilka, H.J. Choi, X.J. Yao, W.I. Weis, R.C. Stevens, B.K. Kobilka, GPCR engineering yields high-resolution structural insights into beta2-adrenergic receptor function, Science 318 (2007) 1266–1273.
[22] J. Standfuss, G. Xie, P.C. Edwards, M. Burghammer, D.D. Oprian, G.F. Schertler, Crystal structure of a thermally stable rhodopsin mutant, J. Mol. Biol. 372 (2007) 1179–1188.
[23] C.B. Roth, M.A. Hanson, R.C. Stevens, Stabilization of the human beta2-adrenergic receptor TM4–TM3–TM5 helix interface by mutagenesis of Glu122(3.41), a critical residue in GPCR structure, J. Mol. Biol. 376 (2008) 1305–1319.
[24] F. Magnani, Y. Shibata, M.J. Serrano-Vega, C.G. Tate, Co-evolving stability and conformational homogeneity of the human adenosine A2a receptor, Proc. Natl. Acad. Sci. U. S. A. 105 (2008) 10744–10749.
[25] M.J. Serrano-Vega, F. Magnani, Y. Shibata, C.G. Tate, Conformational thermostabilization of the beta1-adrenergic receptor in a detergent-resistant form, Proc. Natl. Acad. Sci. U. S. A. 105 (2008) 877–882.
[26] Y. Shibata, J.F. White, M.J. Serrano-Vega, F. Magnani, A.L. Aloia, R. Grisshammer, C.G. Tate, Thermostabilization of the neurotensin receptor NTS1, J. Mol. Biol. 390 (2009) 262–277.
[27] C.A. Sarkar, I. Dodevski, M. Kenig, S. Dudli, A. Mohr, E. Hermans, A. Plückthun, Directed evolution of a G protein-coupled receptor for expression, stability, and binding selectivity, Proc. Natl. Acad. Sci. U. S. A. 105 (2008) 14808–14813.
[28] I. Dodevski, A. Plückthun, Evolution of three human GPCRs for higher expression and stability, J. Mol. Biol. 408 (2011) 599–615.
[29] K.M. Schlinkmann, M. Hillenbrand, A. Rittner, M. Kunz, R. Strohner, A. Plückthun, Maximizing detergent stability and functional expression of a GPCR by exhaustive recombination and evolution, J. Mol. Biol. 422 (2012) 414–428.
[30] K.M. Schlinkmann, A. Honegger, E. Türeci, K.E. Robison, D. Lipovsek, A. Plückthun, Critical features for biosynthesis, stability, and functionality of a G protein-coupled receptor uncovered by all-versus-all mutations, Proc. Natl. Acad. Sci. U. S. A. 109 (2012) 9810–9815.
[31] D.J. Scott, A. Plückthun, Direct molecular evolution of detergent-stable G protein-coupled receptors using polymer encapsulated cells, J. Mol. Biol. 425 (2013) 662–667.
[32] A.S. Dore, N. Robertson, J.C. Errey, I. Ng, K. Hollenstein, B. Tehan, E. Hurrell, K. Bennett, M. Congreve, F. Magnani, C.G. Tate, M. Weir, F.H. Marshall, Structure of the adenosine A(2A) receptor in complex with ZM241385 and the xanthines XAC and caffeine, Structure 19 (2011) 1283–1293.
[33] G. Lebon, T. Warne, P.C. Edwards, K. Bennett, C.J. Langmead, A.G. Leslie, C.G. Tate, Agonist-bound adenosine A2A receptor structures reveal common features of GPCR activation, Nature 474 (2011) 521–525.
[34] T. Warne, R. Moukhametzianov, J.G. Baker, R. Nehme, P.C. Edwards, A.G. Leslie, G.F. Schertler, C.G. Tate, The structural basis for agonist and partial agonist action on a beta(1)-adrenergic receptor, Nature 469 (2011) 241–244.
[35] J. Huang, S. Chen, J.J. Zhang, X.Y. Huang, Crystal structure of oligomeric beta(1)-adrenergic G protein-coupled receptors in ligand-free basal state, Nat. Struct. Mol. Biol. 20 (2013) 419–425.
[36] M. Congreve, R.L. Rich, D.G. Myszka, F. Figaroa, G. Siegal, F.H. Marshall, Fragment screening of stabilized G-protein-coupled receptors using biophysical methods, Methods Enzymol. 493 (2011) 115–136.
[37] J.A. Christopher, J. Brown, A.S. Dore, J.C. Errey, M. Koglin, F.H. Marshall, D.G. Myszka, R.L. Rich, C.G. Tate, B. Tehan, T. Warne, M. Congreve, Biophysical fragment screening of the beta1-adrenergic receptor: identification of high affinity arylpiperazine leads using structure-based drug design, J. Med. Chem. 56 (2013) 3446–3455.
[38] J.D. Pedelacq, S. Cabantous, T. Tran, T.C. Terwilliger, G.S. Waldo, Engineering and characterization of a superfolder green fluorescent protein, Nat. Biotechnol. 24 (2006) 79–88.
[39] J. Tucker, R. Grisshammer, Purification of a rat neurotensin receptor expressed in *Escherichia coli*, Biochem. J. 317 (Pt 3) (1996) 891–899.
[40] R. Grisshammer, P. Averbeck, A.K. Sohal, Improved purification of a rat neurotensin receptor expressed in *Escherichia coli*, Biochem. Soc. Trans. 27 (1999) 899–903.
[41] P. Kitabgi, C. Poustis, C. Granier, J. Van Rietschoten, J. Rivier, J.L. Morgat, P. Freychet, Neurotensin binding to extraneural and neural receptors: comparison with biological activity and structure–activity relationships, Mol. Pharmacol. 18 (1980) 11–19.
[42] P. Kitabgi, C.Y. Kwan, J.E. Fox, J.P. Vincent, Characterization of neurotensin binding to rat gastric smooth muscle receptor sites, Peptides 5 (1984) 917–923.
[43] D. Gully, B. Labeeuw, R. Boigegrain, F. Oury-Donat, A. Bachy, M. Poncelet, R. Steinberg, M.F. Suaud-Chagny, V. Santucci, N. Vita, F. Pecceu, C. Labbe-Jullie, P. Kitabgi, P. Soubrie, G. Le Fur, J.P. Maffrand, Biochemical and pharmacological activities of SR 142948A, a new potent neurotensin receptor antagonist, J. Pharmacol. Exp. Ther. 280 (1997) 802–812.
[44] C. Labbe-Jullie, J.M. Botto, M.V. Mas, J. Chabry, J. Mazella, J.P. Vincent, D. Gully, J.P. Maffrand, P. Kitabgi, [3H]SR 48692, the first nonpeptide neurotensin antagonist radioligand: characterization of binding properties and evidence for distinct agonist and antagonist binding domains on the rat neurotensin receptor, Mol. Pharmacol. 47 (1995) 1050–1056.
[45] C. Labbe-Jullie, S. Barroso, D. Nicolas-Eteve, J.L. Reversat, J.M. Botto, J. Mazella, J.M. Bernassau, P. Kitabgi, Mutagenesis and modeling of the neurotensin receptor NTR1. Identification of residues that are critical for binding SR 48692, a nonpeptide neurotensin antagonist, J. Biol. Chem. 273 (1998) 16351–16357.
[46] S. Barroso, F. Richard, D. Nicolas-Etheve, P. Kitabgi, C. Labbe-Jullie, Constitutive activation of the neurotensin receptor 1 by mutation of Phe(358) in Helix seven, Br. J. Pharmacol. 135 (2002) 997–1002.
[47] Y. Shibata, J. Gvozdenovic-Jeremic, J. Love, B. Kloss, J.F. White, R. Grisshammer, C.G. Tate, Optimising the combination of thermostabilising mutations in the neurotensin receptor for structure determination, Biochim. Biophys. Acta 1828 (2013) 9.
[48] A. Zhukov, S.P. Andrews, J.C. Errey, N. Robertson, B. Tehan, J.S. Mason, F.H. Marshall, M. Weir, M. Congreve, Biophysical mapping of the adenosine A2A receptor, J. Med. Chem. 54 (2011) 4312–4323.